

The Sersic Virial Hyperplane

S.Capozziello¹, V. F. Cardone^{2*}, R. Molinaro², V. Salzano¹

¹ *Dipartimento di Scienze Fisiche, Università degli Studi di Napoli “Federico II” and INFN, Sezione di Napoli, Complesso Universitario di Monte S. Angelo, Via Cinthia, Edificio N, 80126 Napoli, Italy*

² *Dipartimento di Fisica “E.R. Caianiello”, Università di Salerno, Via S. Allende, 84081 - Baronissi (Salerno), Italy*

Accepted xxx, Received yyy, in original form zzz

ABSTRACT

Early - type galaxies (ETGs) are known to possess a number of quite useful scaling relations among their photometric and/or kinematical quantities. We propose a unified picture reducing both the fundamental plane and the photometric plane to suitable projections of a single relation. Modelling the ETG as a two component system, made out of a luminous Sersic profile and a NFW dark halo, and applying the virial theorem, we are able to express the velocity dispersion σ_0 as a function of the effective intensity $\langle I_e \rangle$, the effective radius R_e and the Sersic index n . In a log-log plot, this relation reduces to a hyperplane (i.e., a plane in a four dimensional configuration space) which we dubbed the *Sersic Virial Hyperplane* (SVH). The tilt of the SVH can be fully explained in terms of a power-law scaling of the stellar (rather than the global) mass-to-light ratio Υ_* with the total luminosity L_T , while the scatter is determined by those on the $c - M_{vir}$ relation between the concentration c and the virial mass M_{vir} of the dark halo component. In order to test whether such the observed SVH is consistent with the theoretical assumptions, we perform a detailed simulation of a large ETGs sample reproducing the same photometric properties of a SDSS low redshift ETGs catalog. It turns out that the simulated SVH is fully consistent with the observed one thus validating our theoretical approach.

Key words: galaxies: elliptical and lenticular, cD – galaxies: kinematics and dynamics – galaxies: fundamental parameters – dark matter

1 INTRODUCTION

Elliptical and S0 galaxies (hereafter, collectively referred to as early - type galaxies, ETGs) present a striking regularity in their luminosity distribution. The ETG surface brightness is well fitted by the well known $r^{1/4}$ profile (de Vaucouleurs 1948), while considerable better results are obtained using the Sersic $r^{1/n}$ law (Sersic 1968). From the photometric point of view, therefore, ETG may be considered as characterized by only three parameters, namely the slope n of the Sersic profile, the effective radius R_e containing half of the total luminosity, and the effective surface brightness μ_e defined as $\mu_e = \mu(R_e)$, or equivalently the average surface intensity $\langle I_e \rangle = (L_T/2)/(\pi R_e^2)$.

The ETG kinematic may be schematically characterized through its central velocity dispersion σ_0 which, under suitable assumptions on the mass profile, gives information on the mass and hence the mass-to-light (hereafter M/L) ratio. Being a mass tracer, it is reasonable to expect that σ_0 is somewhat correlated to the total luminosity L_T ,

even if it is difficult to forecast an analytic form for such a correlation, given the subtleties of the luminous and dark components modelling. It is therefore not surprising that empirical searches for such a correlation were early undertaken. A remarkable success was represented by the Faber - Jackson (FJ) $L_T \propto \sigma_0^4$ relation (Faber & Jackson 1976). The large scatter in the FJ law led to the need for higher dimensional representations of ETGs. Considering $n = 4$, there remains just three parameters describing an ETG so that one could wonder whether a relation exist among the photometric quantities ($R_e, \langle I_e \rangle$) and the kinematical σ_0 . This relation were indeed found (Djorgovski & Davis 1987; Dressler et al. 1987) and, when expressed in a logarithmic scale, is just a plane soon dubbed the *fundamental plane* (FP). It is worth noting that such a plane was not unexpected. Indeed, a simple application of the virial theorem gives $R_e \propto \sigma_0^2 \langle I_e \rangle^{-1}$, under the hypotheses of constant M/L ratio and structural homology. The observed FP plane is however tilted, i.e. one indeed finds $R_e \propto \sigma_0^\alpha \langle I_e \rangle^{-\beta}$, but with $(\alpha, \beta) = (1.49, 0.75)$ rather than $(2, 1)$ as forecasted before (Bernardi et al. 2003). Such a tilt may be easily explained introducing a power-law correlation $M/L \propto L_T^\gamma$ (with $\gamma \simeq 0.27$), but interpreting the

* Corresponding author: winny@sa.infn.it.

origin of such a relation is a difficult and ambiguous task due to proposals ranging from non-homology (Prugniel & Simien 1997), to stellar populations effects (Dressler et al. 1987), from systematic variations in kinematical structure (van der Marel 1991; Bender et al. 1992; Busarello et al. 1997) to a combination of different terms (Trujillo et al. 2004).

Although the de Vaucouleurs profile is a satisfactory fit, it is well known that the Sersic profile has to be preferred (Caon et al. 1993; Graham & Colless 1997; Prugniel & Simien 1997). As such, forcing $n = 4$ in the fit may systematically bias the estimate of R_e and $\langle I_e \rangle$ and hence affect the FP. Introducing n increases the number of parameters needed to describe ETGs leading to wonder whether scaling relations exist. Actually, given the observational difficulties in measuring σ_0 , it is worth looking for empirical correlations involving only the photometric parameters. Interesting examples are the Kormendy relation (KR) between R_e and μ_e (Kormendy 1977) and the scalelength-shape relation between R_e and n (Young & Currie 1994). However, just as the FJ relation is a projection of the FP, both the $R_e - \mu_e$ and the $R_e - n$ relations may be seen as projections of a more fundamental law among these three photometric parameters. In logarithmic units, such a relation indeed exists and it is a plane referred to as the *photometric plane* (PhP) recently detected in both near infrared (Khosroshahi et al. 2000) and optical (Graham 2002). While observationally the PhP is confirmed also at intermediate redshift (La Barbera et al. 2004, 2005), a definitive theoretical interpretation is still lacking. Modelling the stars in ETG as a self-gravitating gas, Lima Neto et al. (1999) have recovered a PhP like relation (referred to as the *entropic plane*) by assuming that the specific entropy (i.e., the entropy for mass unit) is constant for all ETGs. Later, Márquez et al. (2001) derived an *energy-entropy* (or *mass-entropy*) line giving a possible explanation for the structural relations among photometric parameters. Moreover, they also find out that the specific entropy increases as a consequence of merging processes so offering a possible way to test the model against the observed variation of the PhP with redshift.

There are two general lessons to draw from the above short summary. First, two dimensional scaling relations turn out to be projections of a more general three dimensional law. It is therefore worth wondering whether this also holds for the FP and PhP being possible projections of a four parameters law. It is worth noting that a first step towards this direction has been attempted by Graham (2002) fitting a hyperplane (in logarithmic units) to the set of parameters $(n, R_e, \langle I_e \rangle, \sigma_0)$, but it was never prosecuted. On the other hand, from a theoretical point of view, both the entropic plane and the FP are tentatively explained on the implicit assumption that ETGs are in a state of dynamical equilibrium so that the virial theorem applies and the Boltzmann-Gibbs entropy may be evaluated. Motivated by these considerations, here we investigate whether a four dimensional relation among photometric and kinematic quantities may come out as consequence of the virial theorem and some assumptions on the stellar M/L consistent with stellar population synthesis models. Should such a relation exist, one could thus reconcile both the FP and the PhP under the same theoretical standard thus representing a valid tool to investigate ETG formation theories.

As a first key ingredient, we describe in Sect. 2 the assumed mass models for both the luminous and the dark components of ETGs. In Sect. 3, we first compute the quantities entering the virial theorem according to the model detailed above and then obtain the four dimensional scaling relation we are looking for. In order to test whether our derivation is consistent with what is observed, we simulate ETG samples that are as similar as possible to a large SDSS based sample following the procedure extensively discussed in Sect. 4. The results of such a testing procedure are described in Sect. 5, while Sect. 6 is devoted to fit our theoretical relation to the observed data using a Bayesian approach. Discussion and conclusions are finally held in Sect. 7.

2 MODELLING ELLIPTICAL GALAXIES

Although some recent results show the presence of thin discs in inner regions of elliptical galaxies[†], ETGs may be well described as a luminous stellar distribution embedded in a dark matter halo dominating the outer mass profile. In the following, we will assume spherical symmetry for both these components. While this is an acceptable hypothesis for the halo, it is clearly an oversimplification for the elliptical luminous component. Nevertheless, this will allow us to get analytical expressions for the main quantities we are interested in without dramatically affecting the main results.

2.1 The Sersic profile

Under the hypothesis of constant M/L , the surface density of the luminous component may be easily obtained as:

$$\Sigma(R) = \Upsilon_* I(R) \quad (1)$$

with Υ_* the M/L ratio and $I(R)$ the surface luminosity density. As well known, the Sersic $r^{1/n}$ law (Sersic 1968) is best suited to describe the surface brightness distribution of elliptical galaxies (Caon et al. 1993; Graham & Colless 1997; Prugniel & Simien 1997). Motivated by these evidences, we will therefore set:

$$I(R) = I_e \exp \left\{ -b_n \left[\left(\frac{R}{R_e} \right)^{1/n} - 1 \right] \right\} \quad (2)$$

with I_e the luminosity density at the effective radius R_e and b_n a constant defined such that the luminosity within R_e is half the total luminosity. It is possible to show that b_n may be found by solving (Ciotti 1991):

$$\Gamma(2n, b_n) = \Gamma(2n)/2 \quad (3)$$

where $\Gamma(a, z)$ is the incomplete Γ function and $\Gamma(a)$ the actual Γ function. Useful approximating formulae may be found in Graham & Driver (2005) and references therein, but we will exactly solve Eq.(3) in the following.

Assuming cylindrical symmetry, the luminosity profile within R is:

[†] S0 galaxies contain, by definition, a thin disc, so that, strictly speaking, our following discussion applies only to the bulge component. However, neglecting this disc does not introduce any significant systematic error. Moreover, our sample is mainly dominated by elliptical galaxies so that we confidently neglect the disc component in S0 systems.

$$L(R) = 2\pi \int_0^R I(R') R' dR' = L_T \times \frac{\gamma(2n, b_n x)}{\Gamma(2n)} \quad (4)$$

with $x \equiv R/R_e$ and

$$L_T = 2\pi n I_e R_e^2 b_n^{-2n} e^{b_n} \Gamma(2n) \quad (5)$$

the total luminosity. The volume luminosity density $j(s)$ may be easily obtained deprojecting $I(R)$. Defining $s = r/R_e$ (with r the radius in spherical coordinates), we get (Mazure & Capelato 2002):

$$\nu(s) = -\frac{1}{\pi} \int_s^\infty \frac{di}{dx} \frac{dx}{\sqrt{x^2 - s^2}}$$

with $i(x) = I(R)/I_e$ and $\nu(s) = (R_e/I_e)j(s)$. Some algebra finally leads to the following expressions for the mass density $\rho_\star(s)$ and the mass profile $M_\star(s)$:

$$\rho_\star(s) = \frac{M_\star^T}{4\pi R_e^3} \times \frac{\mathcal{I}_\nu(s)}{\mathcal{I}_M(s)}, \quad (6)$$

$$M_\star(s) = M_\star^T \times \frac{\mathcal{I}_M(s)}{\mathcal{I}_M(s)}, \quad (7)$$

where we have denoted with M_\star^T the total stellar mass:

$$M_\star^T = 4(b_n/n) \Upsilon_\star I_e R_e^2 \mathcal{I}_M(\infty), \quad (8)$$

having used the abuse of notation

$$f(\infty) = \lim_{y \rightarrow \infty} f(y).$$

Finally, to get Eqs.(6) and (7), we have used the auxiliary functions:

$$\mathcal{I}_\nu(s) = \int_s^\infty \frac{x^{(1-n)/n} \exp[-b_n(x^{1/n} - 1)]}{(x^2 - s^2)^{1/2}} dx, \quad (9)$$

$$\mathcal{I}_M(s) = \int_0^s \mathcal{I}_\nu(s') s'^2 ds'. \quad (10)$$

Both these functions cannot be analytically expressed, but are straightforward to be numerically evaluated.

2.2 The dark halo

Most of the kinematical tracers of the total gravitational potential are usually affected by a severe degeneracy between the luminous component and the dark one so that there are different dark halo models able to fit the same data for a given stellar mass profile. It is therefore important to rely on a physical theory of halo formation to select models which are both compatible with the data and also physically well motivated. From this point of view, numerical simulations of galaxy formation in hierarchical CDM scenarios are very helpful since they predict the initial shape of the dark matter distribution. Here, we assume a NFW profile (Navarro et al. 1997) as initial dark matter halo and neglect the effect of the baryons gravitational collapse. The main features of the NFW model are:

$$\rho_{DM}(r) \equiv \frac{\rho_s}{x(1+x)^2}, \quad x = r/r_s \quad (11)$$

$$M_{DM}(r) = 4\pi \rho_s r_s^3 f(x) = M_{vir} f(x)/f(c), \quad (12)$$

$$f(x) \equiv \ln(1+x) - \frac{x}{1+x}, \quad (13)$$

$$c \equiv r_{vir}/r_s, \quad (14)$$

$$M_{vir} = \frac{4\pi \delta_{th}}{3} \rho_{crit} r_{vir}^3, \quad (15)$$

where c is the concentration parameter, M_{vir} the virial mass and r_{vir} the virial radius[†]. The model is fully described by two independent parameters, which we assume to be c and M_{vir} . Numerical simulations, supported by observational data, motivate a correlation between c and M_{vir} so that the NFW model may be considered as a single parameter family. Following Bullock et al. (2001), we adopt:

$$c = 15 - 3.3 \log(M_{vir} 10^{12} h^{-1} M_\odot) \quad (16)$$

with a log normal scatter $\delta \log c \simeq 0.11$.

The NFW model is not the only model proposed to fit the results of numerical simulations. Some authors (Moore et al. 1998; Ghigna et al. 2000) have proposed models with a central slope steeper than the NFW one. On the other hand, it is also possible that the inner slope does not reach any asymptotic value with the logarithmic slope being a power-law function of the r (Navarro et al. 2004; Cardone et al. 2005) or that the deprojected Sersic profile also fits the numerical dark matter haloes (Merritt et al. 2005; Graham et al. 2006a; Graham et al. 2006b). However, the difference between all these models and the NFW one is very small for radii larger than 0.5% - 1% the virial radius so that we will not consider models other than the NFW one.

3 THE VIRIAL THEOREM

Elliptical galaxies are known to be characterized by scaling relations among their kinematic and structural parameters. In an attempt to investigate whether such empirical laws may be recovered under a single theoretical scheme, we can rely on the hypothesis of statistical equilibrium. In such an assumption, the virial theorem holds:

$$2K + W = 0 \quad (17)$$

with K and W the total kinetic and potential energy respectively. Both these quantities may be evaluated given the assumed spherical symmetry as we detail in the following.

3.1 Kinetic energy

Neglecting the net rotation velocity of the system (which is reasonable, given the low values of v_c in elliptical galaxies), the total kinetic energy is given as (Binney & Tremaine 1987):

$$K = 3\pi \int_0^\infty \Sigma(R) \sigma_p^2(R) R dR \quad (18)$$

with $\Sigma(R)$ the star surface density and $\sigma_p(R)$ the luminosity weighted velocity dispersion projected along the line of sight. For a spherically symmetric system, assuming an isotropic velocity dispersion tensor, it is:

[†] The virial radius is defined such that the mean density within r_{vir} is δ_{th} times the critical density ρ_{crit} . According to the concordance Λ CDM model, we assume a flat universe with $(\Omega_m, \Omega_\Lambda, h) = (0.3, 0.7, 0.72)$ where $\delta_{th} = 337$.

$$\sigma_p^2(R) = \frac{2}{\Upsilon_* I(R)} \int_R^\infty \frac{\rho_*(r) G M_{tot}(r) \sqrt{r^2 - R^2}}{r^2} dr, \quad (19)$$

with $M_{tot}(r) = M_*(r) + M_{DM}(r)$ the total mass profile. As a first step, it is convenient to split the integral in Eq.(19) in two terms separating the dark halo contribution from the luminous one. It is then easy to get :

$$\begin{aligned} \int_R^\infty \frac{\rho_*(r) G M_*(r) \sqrt{r^2 - R^2}}{r^2} dr &= \frac{(M_*^T)^2}{4\pi R_e^3 \mathcal{I}_M(\infty)} \\ &\times \int_R^\infty \frac{\mathcal{I}_\nu(s) \mathcal{I}_M(s)}{s^2 (s^2 - x^2)^{-1/2}} ds, \\ \int_R^\infty \frac{\rho_*(r) G M_{DM}(r) \sqrt{r^2 - R^2}}{r^2} dr &= \frac{M_*^T M_{vir}}{4\pi R_e^3 \mathcal{I}_M(\infty) f(c)} \\ &\times \int_R^\infty \frac{\mathcal{I}_\nu(s) f(s, R_e/r_s)}{s^2 (s^2 - x^2)^{-1/2}} ds, \end{aligned}$$

where $f(s, R_e/r_s)$ is obtained by replacing x with $(R_e/r_s)s$ into Eq.(13). Adding the two terms above and using Eqs.(2) and (8) , we can finally write :

$$\begin{aligned} \sigma_p^2(R) &= \frac{2b_n}{n\pi} \frac{GM_*^T}{R_e} \\ &\times \frac{\mathcal{I}_\sigma^*(x, n) + (M_{vir}/M_*^T) f^{-1}(c) \mathcal{I}_\sigma^{DM}(x, n, R_e/r_s)}{\exp[-b_n (x^{1/n} - 1)]} \end{aligned} \quad (20)$$

with $x = R/R_e$ and :

$$\begin{aligned} \mathcal{I}_\sigma^*(x, n) &\equiv \int_x^\infty \frac{\mathcal{I}_\nu(s) \mathcal{I}_M(s)}{s^2 (s^2 - x^2)^{-1/2}} ds, \\ \mathcal{I}_\sigma^{DM}(x, n, R_e/r_s) &\equiv \int_x^\infty \frac{\mathcal{I}_\nu(s) f(s, R_e/r_s)}{s^2 (s^2 - x^2)^{-1/2}} ds. \end{aligned}$$

As we will see later, $\sigma_p^2(R)$ does not enter the applications we are interested in. It is rather its central value σ_0^2 averaged within a circular aperture of radius $R_e/8$ which is measured by the galaxy spectrum. We therefore evaluate :

$$\sigma_0^2 = \frac{\int_0^{R_e/8} \rho_*(r) M_{tot}(r) [\mathcal{F}_0(R_e/8r) - \mathcal{F}_0(0)] dr}{2 \int_0^{R_e/8} \rho_*(r) [\mathcal{A}_0(R_e/8r) - \mathcal{A}_0(0)] r dr}, \quad (21)$$

with (Dalal & Keeton 2003) :

$$\begin{aligned} \mathcal{F}_0(y) &= \begin{cases} y \sqrt{1 - y^2} + \arcsin y - \pi/2 & y < 1 \\ 0 & y > 1 \end{cases}, \\ \mathcal{A}_0(y) &= \begin{cases} \arcsin y & y < 1 \\ \pi/2 & y > 1 \end{cases}. \end{aligned}$$

When evaluating Eq.(21), we make the simplifying assumptions $M_{tot} \simeq M_*$ since the dark halo mass is negligible with respect to the stellar one over the range interested by the integral. By such an assumption, it is easy to get :

$$\sigma_0^2 = \frac{GM_*^T}{R_e} \times \mathcal{I}_0(n) \quad (22)$$

having defined :

$$\mathcal{I}_0(n) = \frac{1}{\mathcal{I}_M(\infty)} \frac{\int_0^{1/8} \mathcal{I}_\nu(s) \mathcal{I}_M(s) [\mathcal{F}_0(1/8s) - \mathcal{F}_0(0)] ds}{2 \int_0^{R_e/8} \mathcal{I}_\nu(s) [\mathcal{A}_0(1/8s) - \mathcal{A}_0(0)] s ds}. \quad (23)$$

As a next step, we insert Eq.(21) into Eq.(18) and then split the integral in two terms, the first one originated by the product $\Sigma(s) \times \mathcal{I}_\sigma^*(s)$, and the second one due to $\Sigma(s) \times \mathcal{I}_\sigma^{DM}(s)$. By using Eq.(22), we finally obtain :

$$K = \frac{1}{2} M_*^T \sigma_0^2 \times k(\mathbf{p}) \quad (24)$$

with \mathbf{p} denoting the set of parameters

$$\mathbf{p} = (n, R_e, I_e, \Upsilon_*, M_{vir}, c),$$

where we have set :

$$k(\mathbf{p}) = \frac{3}{2} \left[k_*(n, R_e, I_e) + \frac{M_{vir}/M_*^T}{f(c)} k_*^{DM}(n, R_e/r_s) \right], \quad (25)$$

$$k_*(n) = \frac{1}{\mathcal{I}_0(n) \mathcal{I}_M(\infty)} \int_0^\infty \mathcal{I}_\sigma^*(x, n) x dx, \quad (26)$$

$$k_*^{DM}(n, R_e/r_s) = \frac{1}{\mathcal{I}_0(n) \mathcal{I}_M(\infty)} \int_0^\infty \mathcal{I}_\sigma^{DM}(x, R_e/r_s) x dx. \quad (27)$$

Note that, although I_e and Υ_* do not explicitly enter the above equations, they are however included as parameters since they determine the total stellar mass M_*^T because of Eq.(8). On the other hand, r_s is not counted as an independent parameter since it is determined as function of M_{vir} and c . Should we use Eq.(16), the virial mass M_{vir} would be the only parameter related to the dark halo properties.

3.2 The gravitational energy

The computation of W may be carried out in a similar way starting from the definition (Binney & Tremaine 1987) :

$$W = -4\pi G \int_0^\infty \rho_{tot}(r) M_{tot}(r) r dr. \quad (28)$$

Splitting the total density and mass as the sum of the luminous and dark components, after some algebra, one gets :

$$W = -\frac{GM_*^T}{R_e^2} \times w(\mathbf{p}) \quad (29)$$

with \mathbf{p} denoting the same set of parameters as above. The dimensionless quantity $w(\mathbf{p})$ is defined as :

$$\begin{aligned} w(\mathbf{p}) &= w_*(n) \\ &+ \left(\frac{M_{vir}}{M_*^T} \right)^2 \left(\frac{R_e}{r_{vir}} \right) w_{DM}(c) \\ &+ \left(\frac{M_{vir}}{M_*^T} \right) w_*^{DM}(c, n, R_e/r_s) \\ &+ \left(\frac{M_{vir}}{M_*^T} \right) w_{DM}^*(c, n, R_e/r_s). \end{aligned} \quad (30)$$

It is then only a matter of algebra to demonstrate that :

$$w_*(n) = \frac{1}{\mathcal{I}_M^2(\infty)} \int_0^\infty \mathcal{I}_\nu(s) \mathcal{I}_M(s) s ds, \quad (31)$$

$$w_{DM}(c) = \frac{c^2}{f^2(c)} \int_0^\infty \frac{\ln(1 + cy) - cy(1 + cy)^{-1}}{(1 + cy)^2} dy, \quad (32)$$

$$\begin{aligned} w_*^{DM}(c, n, R_e/r_s) &= \frac{1}{\mathcal{I}_M(\infty) f(c)} \\ &\times \int_0^\infty \mathcal{I}_\nu(s) f(s, R_e/r_s) s ds, \end{aligned} \quad (33)$$

$$w_{DM}^*(c, n, R_e/r_s) = \frac{1}{\mathcal{I}_M(\infty)f(c)} \left(\frac{R_e}{r_s}\right)^2 \times \int_0^\infty \left(1 + \frac{R_e}{r_s}s\right) \mathcal{I}_M(s) s ds. \quad (34)$$

It is worth noting that, while n and R_e directly enter the integrals above, Υ_* and I_e only work as scaling parameters through M_*^T . Moreover, a qualitative analysis shows that the first term in Eq.(31) turns out to be the dominating one so that $w(\mathbf{p})$ is essentially a function of n only.

3.3 Scaling relations from the virial theorem

Inserting Eqs.(24) and (29) into Eq.(17) and solving with respect to σ_0 , we get:

$$\sigma_0^2 = \frac{GM_*^T}{R_e} \frac{w(\mathbf{p})}{k(\mathbf{p})}.$$

It is then convenient to introduce:

$$\langle I_e \rangle \equiv \frac{L_T/2}{\pi R_e^2} \quad (35)$$

so that the total stellar mass is $M_*^T = \Upsilon_* L_T = 2\pi \Upsilon_* \langle I_e \rangle R_e^2$ and the relation above can be recast as:

$$2 \log \sigma_0 = \log \langle I_e \rangle + \log R_e + \log \frac{w(\mathbf{p})}{k(\mathbf{p})} + \log (2\pi G \Upsilon_*) . \quad (36)$$

Let us suppose for a while that it is possible to neglect the dark halo component. Should this be the case, both $k(\mathbf{p})$ and $w(\mathbf{p})$ turn out to be a function of $(n, R_e, \langle I_e \rangle)$, where hereafter we use $\langle I_e \rangle$ rather than I_e as a parameter[§]. Although determining how the ratio $w(\mathbf{p})/k(\mathbf{p})$ depends on $(n, R_e, \langle I_e \rangle)$ needs for a full computation of the integrals involved, we can, as first approximation, suppose that $w(\mathbf{p})/k(\mathbf{p})$ is linear in a logarithmic scale. It is possible, therefore, to write:

$$\log [w(\mathbf{p})/k(\mathbf{p})] \simeq a \log \langle I_e \rangle + b \log R_e + c \log (n/4) + d. \quad (37)$$

From stellar population synthesis models, we know that the stellar M/L ratio may be correlated with the total stellar luminosity L_T . Approximating this relation as a power-law, we can therefore write:

$$\log \Upsilon_* \simeq \alpha + \beta \log L_T = \alpha + \beta \log (2\pi \langle I_e \rangle R_e^2). \quad (38)$$

Inserting Eqs.(37) and (38) into Eq.(36), one finally gets:

$$\log \sigma_0 = a_T \log \langle I_e \rangle + b_T \log R_e + c_T \log (n/4) + d_T \quad (39)$$

with

$$\begin{cases} a_T = \frac{a + \beta + 1}{2} \\ b_T = \frac{b + 2\beta + 1}{2} \\ c_T = \frac{c}{2} \\ d_T = \frac{\alpha}{2} + \frac{\beta + 1}{2} \log (2\pi) + \frac{1}{2} \log G + d \end{cases}. \quad (40)$$

[§] See, e.g. Graham & Driver (2005), for the relation between I_e and $\langle I_e \rangle$ and other related formulae.

As a first remark, let us note that the exact value of d depends on the adopted units. In the following, we will express σ_0 in km/s, $\langle I_e \rangle$ in L_\odot/pc^2 and R_e in kpc. In particular, having expressed R_e in linear rather than angular units makes d dependent on the distance to the galaxy. A second important caveat is related to our starting hypothesis of having neglected the dark halo component. Actually, we do know that galaxies are embedded in their dark matter haloes. As a consequence, $w(\mathbf{p})/k(\mathbf{p})$ is a function of the halo parameters too. To take into account this dependence, we still assume Eq.(37), but let d be an unknown function of (c, M_{vir}) to be determined by the data.

With all these caveats in mind, Eq.(39) defines an hyperplane in the logarithmic space allowing to express the kinematic quantity $\log \sigma_0$ as a function of the photometric parameters $\log \langle I_e \rangle$, $\log R_e$, $\log (n/4)$. Since we have recovered it for a Sersic model under the hypothesis of virial equilibrium, we will call it the *Sersic Virial Hyperplane*.

Should our assumptions hold for real elliptical galaxies, the Sersic Virial Hyperplane (hereafter SVH) should represent a tight scaling relations among kinematic and photometric parameters. For an idealized sample of galaxies perfectly satisfying our working hypotheses and all at the same distance, the scatter around this hyperplane should be generated by essentially two terms. First, the halo parameters (c, M_{vir}) may differ on a case-by-case basis. This is the same as saying that the dark matter content in the inner regions or, equivalently, the global M/L ratio (defined as M_{tot}/L_T rather than M_*^T/L_T) is different from one galaxy to another. On the other hand, d_T in Eq.(40) may scatter from one galaxy to another because of different values of the parameters (α, β) of the $\Upsilon_* - L_T$ relation because of different details of the stellar evolution process. Note that this latter effect may also affect the coefficients (a_T, b_T) thus further increasing the scatter on the SVH.

It is worth stressing that the SVH may be seen as a generalization of both the FP and PhP which, from this point of view, reduce to particular cases of the SVH. Indeed, forcing the de Vaucouleurs model to fit the galaxies surface brightness profiles is the same as setting $n = 4$ in Eq.(39). Solving with respect to $\log R_e$, we get:

$$\log R_e = a_{FP} \log \sigma_0 + b_{FP} \log \langle I_e \rangle + c_{FP} \quad (41)$$

which is indeed the FP with

$$\begin{cases} a_{FP} = 1/b_T \\ b_{FP} = -a_T/b_T \\ c_{FP} = -d_T/b_T \end{cases}. \quad (42)$$

Actually, we do not expect that the coefficients of the observed FP are equal to what is predicted by Eq.(42) since, assuming $n = 4$ in the fit, can bias the estimate of $(R_e, \langle I_e \rangle)$ in a way that depends on what the true value of n is. Moreover, the departure of n from $n = 4$ introduces a further scatter which is not included in the above expression for c_{FP} . Although these effects have to be carefully quantified, it is nevertheless worth stressing that the FP turns out to be only a projection of the SVH on the plane $\log (n/4) = 0$ so that its coefficients may be (at least, in principle) predicted on the basis of physical considerations.

On the other hand, when solving Eq.(39) with respect to $\log R_e$, we can also neglect the dependence on $\log \sigma_0$ assuming this latter is, in a rough approximation, the same for all galaxies. We thus get :

$$\log R_e = a_{PhP} \log \langle I_e \rangle + b_{PhP} \log (n/4) + c_{PhP} \quad (43)$$

with

$$\begin{cases} a_{PhP} = -a_T/b_T \\ b_{PhP} = -c_T/b_T \\ c_{PhP} = (1/b_T) \log \sigma_0 - d_T/b_T \end{cases} \quad (44)$$

which is indeed the PhP. Note that, since $\log \sigma_0$ is obviously not the same for all galaxies, the scatter in the PhP may then be easily interpreted as a scatter in $\log \sigma_0$ and hence in the kinematic structure of the galaxies.

4 TESTING THE SVH

The derivation of the SVH in Eq.(39) relies on two main hypothesis which are analytically formalized in Eqs.(37) and (38). While the relation $\Upsilon_* \propto L_T^\beta$ may be tested resorting to stellar population synthesis models, checking the validity of Eq.(37) needs for a detailed computation of $w(\mathbf{p})/k(\mathbf{p})$ as function of the photometric parameters ($n, \langle I_e \rangle, R_e$), the stellar M/L ratio Υ_* and the halo parameters (c, M_{vir}). Performing such a computation over a fine grid in this six dimensional space is prohibitively expensive. We can however rely on a different and more reliable approach. Rather than evaluating $w(\mathbf{p})/k(\mathbf{p})$, we simulate a sample of galaxies with given values of the above parameters and use the set of equations in Sect.3 to compute σ_0 and the ratio $w(\mathbf{p})/k(\mathbf{p})$. We thus end up with a sample of *simulated measurements* of $(\sigma_0, n, \langle I_e \rangle, R_e)$ which we fit with the SVH thus determining the coefficients $(a_{sim}, b_{sim}, c_{sim}, d_{sim})$. Let us then assume that our simulated sample have the same distribution for the parameters ($n, \langle I_e \rangle, R_e, \Upsilon_*$) as a real sample. Let us then denote with $(a_{obs}, b_{obs}, c_{obs}, d_{obs})$ the values obtained by fitting the SVH to the observed sample. Should our assumptions be satisfied, we have to find :

$$\begin{cases} a_{obs} = a_{sim} + \beta/2 \\ b_{obs} = b_{sim} + \beta \\ c_{obs} = c_{sim} \\ d_{obs} = d_{sim} + \alpha/2 + (\beta/2) \log (2\pi) \end{cases} \quad (45)$$

with β an estimate of the slope of the $\Upsilon_* - L_T$ relation. Moreover, the scatter in the observed SVH should be the same as the one evaluated by the simulated sample. Actually, since we do not have a model independent guess for β , we can estimate β as $2(a_{obs} - a_{sim})$ or as $b_{obs} - b_{sim}$. The two estimates thus obtained should of course be equal thus giving a further check on the validity of the model.

4.1 The data

In order to carry on the approach detailed above, a key step is a sample of ETGs as large as possible. To this aim, we

have started from the NYU Value-Added Galaxy Catalog (hereafter, VAGC) which is a cross-matched collection of galaxy catalogs maintained for the study of galaxy formation and evolution (Blanton et al. 2005) and mainly based on the SDSS data release 4 (Adelman-McCarthy et al. 2006). Among the vast amount of available data, we use the *low-redshift* (hereafter, lowZ) catalog of galaxies with estimated comoving distances in the range $10 < d < 150 h^{-1} \text{Mpc}$. We refer the reader to Blanton et al. (2005) and the VAGC website[¶] for details on the compilation of the catalog^{||}.

We shortcut the lowZ catalog only retaining those data we are mainly interested in and rejecting all the galaxies with no measurements of σ_0 leaving us with 24387 out of 28089 objects with magnitudes in the five SDSS filters $u'g'r'i'z'$. In order to select only ETGs, we apply a set of criteria which we briefly details below.

(i) A Sersic profile has been fitted to the surface brightness profile of each galaxy using an automated pipeline retrieving the parameters (n, R_e, A) with R_e in *arcsec* and A the total flux in nanomaggies. As a first criterium, we select only galaxies with $2.5 \leq n \leq 5.5$, where the upper limit is dictated by the code limit $n = 6.0$. This selection is performed using the fit in the i' band since it is less affected by dust without the reduced efficiency of the z' band.

(ii) As a second criterium, we impose the cut $R_{90}/R_{50} > 2.6$ (Shimasaku et al. 2001) with R_{90} and R_{50} the Petrosian radii containing 90% and 50% of the total luminosity as estimated by the data. Note that, although the Petrosian radii do non depend on any fitting, the ratio R_{90}/R_{50} is correlated with n so that the two criteria are somewhat redundant. Removing one of them or changing the order does not alter in a significant way the final sample.

(iii) We exclude all galaxies with $\sigma_0 < 70 \text{ km/s}$ since the dispersion velocity measurements for these systems may be problematic (Bernardi et al. 2005).

(iv) Elliptical galaxies are segregated in a well defined region of the color-magnitude plane. In order to further restrict our sample, we therefore impose the cut $(g-r)_- \leq g-r \leq (g-r)_+$ with $(g-r)_\pm = pM_r + q \pm \delta$. Here, M_r is the absolute magnitude in the r filter and the parameters (p, q, δ) have been tailored from Fig.2 in Bernardi et al. (2005) where a different ETG sample has been extracted from the SDSS DR2.

The final sample thus obtained contains 5142 galaxies out of an initial catalog containing 24387 objects. It is worth noting that most of the rejected objects have been excluded by the first three cuts (retaining only 5172 entries), while the fourth cut only removes 30 further galaxies. This is reassuring since the last cut is somewhat qualitative and based on a different set of selection criteria^{**} (Bernardi et al. 2005).

We then use the data reported in the lowZ catalog for

[¶] <http://sdss.physics.nyu.edu/vagc/>

^{||} Note that the version we are using is updated only to the second SDSS data release (Abazajian et al. 2004) covering an effective survey area of 2220.9 square degrees.

^{**} It is worth noting that we cannot use these criteria since the lowZ catalog does not report the parameters which the selection by Bernardi et al. (2005) are based on.

the galaxies in the above sample to collect the quantities listed below.

- *Photometric quantities.* While the Sersic index n and the effective radius R_e in *arcsec* are directly available in the lowZ catalog, the average effective intensity $\langle I_e \rangle$ is not present. To this aim, we first convert the total flux A (in nanomaggies) reported in the catalog in the apparent total magnitude m_t as (Blanton et al. 2005):

$$m_t = 22.5 - 2.5 \log A.$$

We then use the assumed concordance cosmological model to estimate the total absolute magnitude \mathcal{M}_t as:

$$\begin{aligned} \mathcal{M}_t &= m_t - 5 \log D_L(z) + 5 \log h - 10 \log(1+z) \\ &- K(z) - A_G - 42.38 \end{aligned}$$

where z is the galaxy redshift, D_L the luminosity distance, $K(z)$ the K -correction, A_G the galactic extinction, and the term $10 \log(1+z)$ takes into account the cosmological dimming. While $K(z)$ and A_G are reported in the catalog for each of the five SDSS filters, our use of the luminosity distance makes the estimate of M_t cosmological model dependent. However, for the values of z involved, the dependence on the cosmological model is actually meaningless. We finally estimate:

$$\langle I_e \rangle = 10^{-6} \times \frac{\text{dex}[(\mathcal{M}_t - \mathcal{M}_\odot)/2.5]}{2\pi R_e^2} \quad (46)$$

with $\text{dex}(x) \equiv 10^x$, \mathcal{M}_\odot the Sun absolute magnitude in the given filter^{††}. We stress that, in Eq.(46), R_e is expressed in *kpc* rather than *arcsec*. To this aim, we simply use:

$$R_e(\text{kpc}) = R_e(\text{arcsec}) \times D_A(z)/206265$$

with $D_A(z)$ the angular diameter distance in Mpc.

- *Kinematic quantities.* The lowZ catalog reports the velocity dispersion and its error as determined from the SDSS spectrum of the galaxy. This is measured in a circular aperture of fixed radius $R_{ap} = R_{SDSS} = 1.5 \text{ arcsec}$, while σ_0 in Eq.(22) has been estimated for $R_{ap} = R_e/8$. To correct for this offset, we follow Jørgensen et al. (1995, 1996) setting:

$$\sigma_0^{obs} = \sigma_0^{lowZ} \times \left(\frac{R_{SDSS}}{R_e/8} \right)^{0.04} \quad (47)$$

with σ_0^{lowZ} the value in the catalog and R_e in *arcsec* here.

- *Auxiliary quantities.* The lowZ catalog contains a wealth of information on each object that we really do not need for our analysis. We do, however, add to our catalog some further quantities that we will use for check. In particular, we include the absolute magnitude \mathcal{M}_{SDSS} as estimated from the image rather than the fit, and the average effective surface brightness computed as (Graham & Driver 2005):

$$\langle \mu_e \rangle = \langle \mu_e \rangle_{abs} + 10 \log(1+z) + K(z) + A_G$$

with

$$\langle \mu_e \rangle_{abs} = \mathcal{M}_t + 2.5 \log(2\pi R_e^2) + 36.57$$

^{††} We use $\mathcal{M}_\odot = (5.82, 5.44, 4.52, 4.11, 3.89)$ for the $u'g'r'i'z'$ filters respectively as evaluated from a detailed Sun model reported in www.ucolick.org/~cnaw/sun.html

with R_e in *kpc*. Note that $\langle \mu_e \rangle$ rather than $\log \langle I_e \rangle$ is often used in the FP and PhP fit.

Although the Sersic law is known to well fit the surface brightness profile of ETGs, it is worth noting that our derivation of $\langle I_e \rangle$ relies on extrapolating the fit results well beyond the visible edge of the galaxy. As such, it is possible that \mathcal{M}_t provides a biased estimate of the actual total absolute magnitude of the galaxy which is better represented by \mathcal{M}_{SDSS} . A bias in the estimate of \mathcal{M}_t propagates on the estimates of the colors which may be related to the stellar mass by population synthesis models. In order to reduce as more as possible such a bias, we have studied the histogram of $\Delta col = col_{obs} - col_{est}$, where $col_{obs} = \mathcal{M}_{SDSS,j} - \mathcal{M}_{SDSS,k}$ and $col_{est} = \mathcal{M}_{t,j} - \mathcal{M}_{t,k}$. In principle, all these histograms should be centered at the null value with a small scatter. After removing 42 outliers, this is indeed the case for $g' - r'$ and $r' - i'$ (with rms values of 0.08 and 0.06 mag respectively), while this is not for $u' - r'$ and $i' - z'$ (having rms values of 0.21 and 0.13 mag). Motivated by this bias, we will use only data in $g'r'i'$ filters when fitting the SVH taking, in particular, the results from the fit to the i' band as the fiducial ones.

4.2 The simulated sample

The approach we have outlined above to test the validity of the SVH (and, hence, of the hypotheses it relies on) is the construction of simulated sample of ETG which is as similar as possible to the real one. In particular, the photometric parameters of the simulated sample should match as closely as possible those of the observed one.

To this aim, we first look at the histograms of the Sersic parameters $(n, R_e'', \log \langle I_e \rangle)$ with R_e'' the effective radius in *arcsec*, the effective radius R_e in *kpc*, and the distance modulus dm computed as:

$$\begin{aligned} dm &= 5 \log D_L(z) - 5 \log h + 10 \log(1+z) \\ &+ K(z) + A_G + 42.38. \end{aligned}$$

Note that all the quantities entering the definition above are available for each galaxy in the lowZ catalog so that the distribution of dm values is easily obtained. We use the i' values as fiducial ones and start from the histogram thus obtained to compute the cumulative distribution functions (CDF) for the quantities of interest. A simulated galaxy is then generated according to the steps we sketch below.

- Using the CDFs obtained above, we generate the i' values of the parameters $(n, R_e'', \log \langle I_e \rangle, R_e, dm)$. It is worth stressing that the ratio R_e''/R_e provide an estimate of the angular diameter distance $D_A(z)$ to the simulated galaxy and, hence, of the redshift provided a cosmological model has been set. As an alternative approach, one could generate the redshift z and R_e to infer R_e'' . Although the two approaches are in principle equivalent, we have checked that our choice is more stable from a computational point of view. Note also that generating dm directly makes it possible to avoid deriving an estimate for $K(z)$ and A_G thus reducing the number of quantities to be generated.
- The parameters we have generated are given in the i'

filter^{‡‡}, while we would like to simulate the galaxy properties in all the observed filters. To this aim, we have verified that linear relations between the parameters in different filters exist in the real sample so that we can write :

$$\mathbf{p}_f = \mathcal{A}\mathbf{p}_{i'}$$

with \mathbf{p}_f the set of parameters $(n, R_e'', \log \langle I_e \rangle, R_e, dm)$ in the f filter and \mathcal{A} a diagonal matrix. Using this relations, we then generate the values of \mathbf{p}_f for the simulated galaxy in the remaining $u'g'r'z'$ filters. We are now able to compute all the described photometric and auxiliary quantities in the case of the real sample.

iii. As a last step, we need to compute the velocity dispersion σ_0 and its error considering the ETG modelling described in Sect. 2. To this aim, we need to generate three further quantities, namely the stellar M/L ratio Υ_* and the NFW parameters (c, M_{vir}) . As a first step, we construct the CDF for Υ_* from the real sample. To this aim, for each observed galaxy, we estimate (Fukugita et al. 1998) :

$$\Upsilon_*^V = 4.0 + 0.38 [t(z) - 10] \quad (48)$$

with $t(z)$ the age (in Gyr) of the galaxy at redshift z computed assuming a formation redshift $z_F = 2$. We then convert to the i' band M/L as :

$$\log \Upsilon_* = \log \Upsilon_*^V + 0.4 \left[(V - i') - (V - i')_\odot \right] \quad (49)$$

with $V - i' = 0.79$ (Fukugita et al. 1995). The CDF thus obtained is then used as seed for the random generation of the simulated galaxy Υ_* . We can then estimate the total stellar mass M_*^T as $2\pi\Upsilon_*R_e^2\langle I_e \rangle$. In order to set the halo model parameters, we first generate the fraction of the total galaxy mass represented by the dark matter. Defining $\eta = M_{vir}/(M_*^T + M_{vir})$, we extract η from a Gaussian distribution centred on 0.90 and with dispersion 0.03. It is then a simple algebra to find out $M_{vir} = \eta/(1 - \eta) \times M_*^T$ so that we have only to choose a value for the concentration c . To this aim, we use Eq.(16) to set the centre of a Gaussian distribution for c with a dispersion of 0.11 dex. Since the model is then fully assigned, we may resort to Eq.(22) to estimate σ_0 and to Eqs.(24) and (29) to compute $k(\mathbf{p})$ and $w(\mathbf{p})$. The error on the predicted σ_0 is finally set as $\varepsilon\sigma_0$ with ε extracted from a CDF obtained by the same distribution as the observed one.

We repeat the procedure outlined above $\mathcal{N} \simeq 10000$ times thus obtaining a simulated sample to which we apply the same selection procedure as for the real data. We finally end up with a simulated sample containing (approximately) the same number of ETGs as the real one. While, by construction, the distribution of the photometric parameters $(n, R_e, \langle I_e \rangle)$ is the same as the observed one in the i' filter, we have checked that the same applies in the other filters. Moreover, we have checked that the statistical distributions of m_t and \mathcal{M}_t and of the colors are the same as the observed ones. We are therefore confident that the simulated sample is a fair representation of the real data thus making sense to use it as input for testing the SVH as described above.

^{‡‡} Note that dm depends on the filter used because of the terms $K(z)$ and A_G that are wavelength dependent.

5 RESULTS

The real and the simulated samples described above are the input ingredients for the procedure used to test the SVH. As a preliminary step, however, we have to choose a method to fit the SVH to a given dataset. As well known (Feigelson & Babu 1996; Akritas & Bershady 1996; La Barbera et al. 2000), fitting a linear relation in a multiparameter space may seriously depend on the method adopted to get the estimate of the coefficients. Moreover, the choice of the most suitable method also depends on the uncertainties on the model parameters. In the present case, there is a further complication since the lowZ catalog does report the measurement uncertainties on σ_0 , but not on the photometric parameters. As such, we have therefore decided to consider σ_0 as the dependent variable and neglect, in a first approximation, the measurement errors. We therefore use a *direct fit* approach, i.e. we minimize :

$$\chi^2 = \sum_{i=1}^{\mathcal{N}_{obs}} \left[(\log \sigma_0)_{i,obs} - (\log \sigma_0)_{i,SVH} \right]^2 \quad (50)$$

where $(\log \sigma_0)_{i,obs}$ and $(\log \sigma_0)_{i,est}$ are respectively the observed value and the predicted one through the SVH (39) for the i -th galaxy and the sum is over the \mathcal{N}_{obs} elements in the (observed or simulated) sample. We estimate the parameters (a, b, c, d) by minimizing the χ^2 defined above with an iterative 1.5σ -clipping rejection scheme^{§§}. The root mean square of the fit residuals is then taken as an estimate of the intrinsic scatter around the SVH.

An important remark is in order. Although one may question on what fitting procedure is the most suitable one, we stress that we are here mainly interested in testing the consistency between what data effectively mean and what our theoretical assumptions predict. To this aim, it is more important that both the observed and the simulated samples are examined in the same way rather than discussing on which method is the best one. We are therefore confident that the choice of the direct fit approach does not alter the main conclusions we will draw from the comparison among the observed and predicted SVH coefficients and scatter.

As a final warning, note that in the rest of this section, we only consider data and simulations carried out in the i' filter in order to avoid any bias from our qualitative generation of the galaxy properties in other filters. We have however checked that the main results are unchanged should we use the g' or r' filters. Moreover, we only report numerical values of one fiducial simulated sample. However, averaging over different simulations has no significant effect on the results.

5.1 The linear relation hypothesis

As a first fundamental hypothesis in deriving the SVH from the virial theorem, we have assumed that the ratio $w(\mathbf{p})/k(\mathbf{p})$ is log-linear in the photometric parameters $(n, R_e, \langle I_e \rangle)$. With the simulated sample at hand, we may

^{§§} The σ -clipping procedure retains more than 85% of the data. The direct fit with no σ -clipping leads to consistent estimates of the SVH parameters, but the scatter turns out to be artificially increased because of clear outliers.

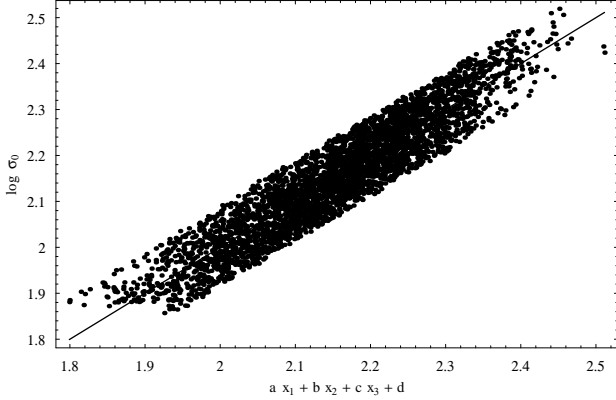


Figure 1. On the y -axis, $\log \sigma_0$ is reported as observed for the ETG sample. On the x -axis, the same quantity is reported as fitted by the linear relation $ax_1 + bx_2 + cx_3 + d$ with $x_1 = \log \langle I_e \rangle$, $x_2 = \log R_e$, $x_3 = \log (n/4)$. The coefficients (a, b, c, d) are estimated by a direct fit as explained in the text.

check whether this is indeed the case. To this aim, we have used the direct fit approach fitting Eq.(37) to the values of $\log [w(\mathbf{p})/k(\mathbf{p})]$ computed for the galaxies in the simulated sample. We find a linear relation among $y = \log [w(\mathbf{p})/k(\mathbf{p})]$ and $x = a \log \langle I_e \rangle + b \log R_e + c \log (n/4) + d$ thus validating Eq.(37). For the simulation reported, we find^{¶¶}:

$$(a, b, c) \simeq (-0.05, 0.04, 0.29)$$

with an intrinsic scatter $\sigma_{int} \simeq 0.08$. Using such values and Eq.(40) with $\beta = 0$, we then estimate:

$$(a_T, b_T, c_T) \simeq (0.48, 0.52, 0.14) .$$

Should our ETG modelling and the virial theorem apply, we then expect that the SVH in Eq.(39) with (a, b, c) fits the observed data reasonably well. On the one hand, we have not used any $\Upsilon_\star - L_T$ relation (that is why we have set $\beta = 0$ above) when computing $w(\mathbf{p})/k(\mathbf{p})$ and σ_0 . However, stellar population synthesis (SPS) models suggest that such a relation indeed exists. One can, in principle, use a SPS code to get an estimate of (α, β) , but this should introduce a further set of assumptions (such as, e.g., star formation history, metallicity, internal absorption) needed as input for the code itself. In order to escape these problems, we have therefore decided to follow a different strategy solving Eqs.(45) with respect to (α, β) , using as input the observed and predicted values of the SVH parameters. Note that, since β may be solved from two different equations, this will offer also a consistency check for the theory.

5.2 The SVH coefficients

In order to test definitively our hypotheses, we first fit the SVH to the observed data using the direct fit approach outlined above. The result is shown in Fig. 1 where we plot y vs x with $y = \log \sigma_0$ and x as above, finding

$$(a_{obs}, b_{obs}, c_{obs}, d_{obs}) = (0.493, 0.640, 0.145, 0.754) \quad (51)$$

^{¶¶} We are not concerned now with the value of d since this also depends on the average distance of the galaxies sample.

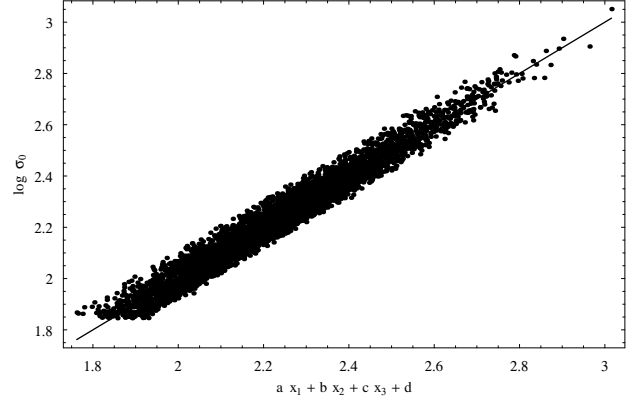


Figure 2. On the y -axis, we report $\log \sigma_0$ as computed for the simulated ETG sample. On the x -axis, we instead report the same quantity as fitted by the linear relation $ax_1 + bx_2 + cx_3 + d$ with $x_1 = \log \langle I_e \rangle$, $x_2 = \log R_e$, $x_3 = \log (n/4)$. The coefficients (a, b, c, d) are estimated from a direct fit as explained in the text.

with an intrinsic scatter $\sigma_{int}^{obs} = 0.045$. As Fig. 1 clearly shows, the SVH fits the data remarkably well over the full observed range in $\log \sigma_0$. The fit residuals are quite small and do not correlate neither with x nor with y . We can therefore safely conclude that the SVH is indeed observationally well founded^{|||}.

Motivated by these encouraging result, we now turn to the simulated sample repeating the same fit as above, but with y now computed on the basis of our ETG modelling and assumptions on the halo parameters. Fig. 2 clearly shows that the SVH fits very well the simulated data with:

$$(a_{sim}, b_{sim}, c_{sim}, d_{sim}) = (0.475, 0.515, 0.142, 0.822) \quad (52)$$

with an intrinsic scatter $\sigma_{int}^{sim} = 0.040$. Comparing Eq.(51) and (52) is a rewarding task. Indeed, c_{obs} and c_{sim} are remarkably close which is exactly what we do expect because of Eq.(40). Moreover, the scatter is quite similar with a modest underestimate ($\Delta\sigma_{int} = \sigma_{int}^{obs} - \sigma_{int}^{sim} = 0.05$). Considering that we have included as source of the scatter only the one due to the $c - M_{vir}$ relation and neglected that introduced by the conversion from Υ_\star^V to Υ_\star , such a small value of $\Delta\sigma_{int}$ has not to be considered as a shortcoming of our theoretical assumptions.

Solving Eq.(45) with respect to β using the values of a_{obs} and a_{sim} gives $\beta \simeq 0.03$, while $\beta \simeq 0.12$ is obtained from b_{obs} and b_{sim} . These two estimates are not consistent with respect to each other so that one could be tempted to conclude that something is wrong with our hypotheses. There are however some important systematic errors which these difference could be ascribed to. First, we stress that the values in Eq.(52) have been obtained from a simulated ETG

^{|||} It is worth noting that a first attempt to fit a hyperplane to a small sample of Coma and Fornax galaxies (collected from the literature available at that time) has yet been successfully performed in Graham (2005). However, in that work, the fit was only empirically motivated and the rest of the paper gives off the dependence on σ_0 concentrating on the PhP. We can therefore consider the present work as the first theoretically motivated study of the SVH based on a large and homogenous ETG sample.

sample obtained under the simplifying hypothesis of spherical symmetry. As well known (Binney & Tremaine 1987), for a given total mass, the velocity dispersion may considerably differ between spherically and flattened systems. As a second simplification, we have computed the kinetic energy in the case of isotropy in the velocity space, while it is likely that ETGs are anisotropic systems. Quantifying these effects is not possible unless one takes carefully into account the distribution in the intrinsic flattening q and the anisotropy parameter β_σ which are largely unknown. We can roughly quantify the effect of these systematics errors by first writing the *true* velocity dispersion as :

$$\sigma_{0,true}^2 = \sigma_0^2 + \sigma_{0,sys}^2 = \sigma_0^2 \times \left[1 + \left(\frac{\sigma_{0,sys}}{\sigma_0} \right)^2 \right]$$

with $\sigma_{0,sys}$ the term we are neglecting due to the systematic errors above. Using the SVH for σ_0^2 , we get :

$$\begin{aligned} \log \sigma_{0,true} &= a_T \log \langle I_e \rangle + b_T \log R_e + c_T \log (n/4) + d_T \\ &+ \frac{1}{2} \log \left[1 + \left(\frac{\sigma_{0,sys}}{\sigma_0} \right)^2 \right]. \end{aligned} \quad (53)$$

The fit to the real data is consistent with the existence of the SVH so that we can argue that the last term on the r.h.s. is linear in logarithmic units. In particular, by writing

$$\log \left[1 + \left(\frac{\sigma_{0,sys}}{\sigma_0} \right)^2 \right] = \delta \log \langle I_e \rangle \quad (54)$$

the SVH is recovered provided that we replace a_T with $a_T + \delta/2$. The matching between simulated and observed coefficients is now obtained for :

$$\begin{cases} a_{sim} + \beta/2 + \delta = a_{obs} \\ b_{sim} + \beta = b_{obs} \end{cases} \quad (55)$$

From the values of $(a_{obs}, b_{obs}, a_{sim}, b_{sim})$, we thus get :

$$(\beta, \delta) \simeq (0.12, -0.09) .$$

It is worth noting that such a small value of β indicates a quite weak correlation between Υ_\star and L_T . This is qualitatively consistent with the finding of Padmanabhan et al. (2004). Estimating the stellar M/L from the correlation with the D_{4000} strength (Kauffman et al. 2003), these authors find Υ_\star to be almost constant with L_T which compares well with our estimated β . Moreover, defining the dynamical mass M_{dyn} as the total mass within (approximately) R_e and estimating it as $M_{dyn} = (1.65)^2 \sigma_0^2 R_e / G$, Padmanabhan et al. finds $M_{dyn}/L_T \propto L_T^{0.17}$. With our finding $\Upsilon_\star \propto L_T^{0.12}$, we can recover the Padmanabhan et al. result provided $M_{dyn}/M_\star^T \propto L_T^{-0.04}$. Using the real data and estimating Υ_\star from Eq.(48), we find $M_{dyn}/M_\star^T \propto L_T^{0.03}$ so that our model predicts $M_{dyn}/L_T \propto L_T^{0.15}$ in remarkable agreement with the Padmanabhan et al. value.

Notwithstanding the encouraging result for β , it is worth stressing that Eq.(54) is actually an unmotivated assumption. Nevertheless, we can qualitatively assess whether such a hypothesis is reasonable by a qualitative analogy with spiral galaxies. Some recent works (Roscoe 1999; Noordermeer et al. 2007) claims that the shape of the rotation curve is determined not only by the total luminosity, but also weakly depends on the mean surface density. Considering σ_0

as the analog of v_c for ETGs, we may qualitatively assume that the power-law relation $\Upsilon_\star - L_T$ describes the dependence of $\sigma_{0,true}$ on L_T , while Eq.(54) takes into account a possible effect related to $\langle I_e \rangle$. Although this interpretation is, strictly speaking, unmotivated, the low δ value and the positive match with the Padmanabhan et al. finding make us confident that Eq.(54) is not unrealistic.

Considering these encouraging results, we therefore conclude that the theoretically predicted SVH can reasonably coincide with the observational one.

6 THE OBSERVED SVH

In the previous section, we were mainly interested in testing the theoretical bases of SVH so that what is pressing is the need for a consistent and homogenous analysis of both the observed and the simulated data. Such a consideration has motivated our choice of the simplified fitting method which is, however, not best suited to derive the *true* SVH coefficients. In particular, we have not taken into account the measurement uncertainties on σ_0 giving the same weight to each ETG in the sample. Moreover, the scatter in the SVH has been estimated *a posteriori*, while one should more correctly take into account such an intrinsic scatter *a priori*, i.e. as a further parameter to be determined by the fitting procedure.

The Bayesian probabilistic approach offers an ideal route to solve this problem. We do not enter in any detail here referring the interested reader to the vast literature available (see, e.g., D'Agostini (2004) and refs. therein). Let us suppose that a linear relation holds as :

$$y = ax_1 + bx_2 + cx_3 + d \quad (56)$$

and let σ_{int} be its intrinsic scatter. If the errors on the variables involved are statistically independent, one can demonstrate that the best fit estimate of the parameters (a, b, c, d) and of the scatter σ_{int} is obtained by minimizing the following merit function (D'Agostini 2005) :

$$\begin{aligned} -\ln \mathcal{L} &= \frac{1}{2} \sum_{i=1}^N \ln (\sigma_{int}^2 + \sigma_{y,i}^2 + a^2 \sigma_{1,i}^2 + b^2 \sigma_{2,i}^2 + c^2 \sigma_{3,i}^2) \\ &+ \frac{1}{2} \sum_{i=1}^N \frac{(y_i - ax_{1,i} - bx_{2,i} - cx_{3,i} - d)^2}{\sigma_{int}^2 + \sigma_{y,i}^2 + a^2 \sigma_{1,i}^2 + b^2 \sigma_{2,i}^2 + c^2 \sigma_{3,i}^2} \end{aligned} \quad (57)$$

with $\sigma_{y,i}$ and $\sigma_{j,i}$ the errors on y and x_j for the i -th object and the sum is over the N objects in the sample. It is worth stressing that the minimization with respect to d may be performed analytically, i.e., for given (a, b, c, σ_{int}) , the best fit d is given by :

$$d = \frac{\sum_{i=1}^N \frac{y_i - ax_{1,i} - bx_{2,i} - cx_{3,i}}{\sigma_{int}^2 + \sigma_{y,i}^2 + a^2 \sigma_{1,i}^2 + b^2 \sigma_{2,i}^2 + c^2 \sigma_{3,i}^2}}{\sum_{i=1}^N \frac{1}{\sigma_{int}^2 + \sigma_{y,i}^2 + a^2 \sigma_{1,i}^2 + b^2 \sigma_{2,i}^2 + c^2 \sigma_{3,i}^2}} \quad (58)$$

With this value of d , one can compute $-\ln \mathcal{L}$ and then find the set of parameters $(a, b, c, d, \sigma_{int})$ that minimizes it, therefore representing the best fit solution.

The general formulae (56) – (58) may be easily adapted to our problem. Eqs.(39) and (56) may be identified setting :

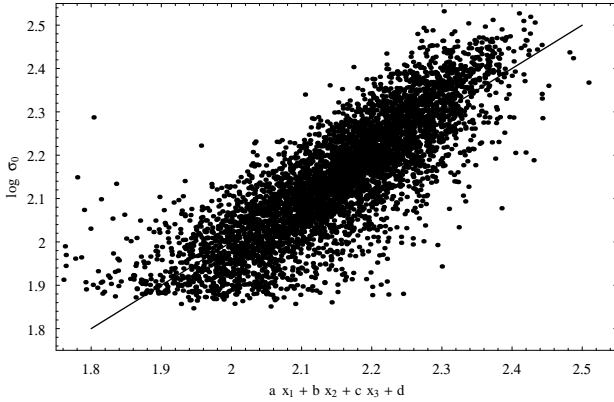
$$y = \log \sigma_0, \quad x_1 = \log \langle I_e \rangle, \quad x_2 = \log R_e, \quad x_3 = \log (n/4) .$$

Table 1. Best fit coefficients and intrinsic scatter of the SVH in the $g'r'i'$ filters obtained as described in the text.

Filter	a	b	c	d	σ_{int}
g'	0.433 ± 0.008	0.595 ± 0.010	0.102 ± 0.014	0.880 ± 0.022	0.089 ± 0.002
r'	0.460 ± 0.008	0.600 ± 0.010	0.113 ± 0.014	0.841 ± 0.022	0.081 ± 0.002
i'	0.469 ± 0.008	0.594 ± 0.010	0.146 ± 0.014	0.824 ± 0.022	0.077 ± 0.003

Table 2. Best fit coefficients and intrinsic scatter of the SVH as rewritten in Eq.(59) in the $g'r'i'$ filters.

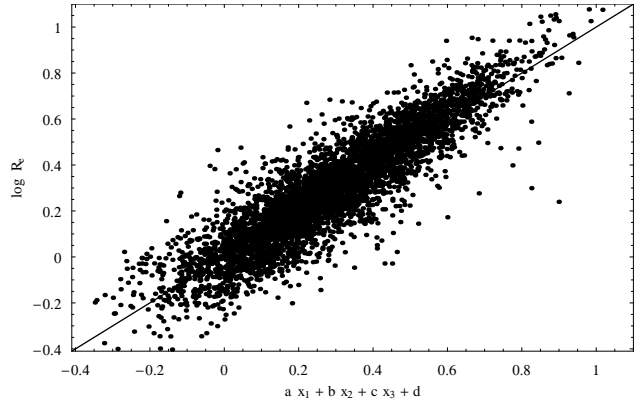
Filter	a_e	b_e	c_e	d_e	$\sigma_{int,e}$
g'	0.897 ± 0.020	-0.659 ± 0.007	0.064 ± 0.022	0.052 ± 0.039	0.110 ± 0.002
r'	0.973 ± 0.022	-0.678 ± 0.008	0.076 ± 0.023	-0.111 ± 0.039	0.100 ± 0.002
i'	1.020 ± 0.020	-0.695 ± 0.007	0.052 ± 0.021	-0.189 ± 0.036	0.100 ± 0.003


Figure 3. Same as Fig. 1 but with the fit coefficients estimated from the Bayesian method.

Note that, for the data at hand, $\sigma_1 = \sigma_2 = \sigma_3 = 0$. Finally, we find the results summarized in Table 1 for the SVH in the $g'r'i'$ filters (excluding therefore the u' and z' data for the problems hinted to in Sect. 4) where the errors on the fit parameters have been estimated by 1000 bootstrap resampling. Fig. 3 gives a visual impression of the quality of the fit superimposing the best fit curve to the i' filter data.

Comparing the results in Table 1 for the i' filter and those in Eq.(51), we find a good agreement for both c and d coefficients, while a less good but still reasonable matching is obtained for a and b . From this point of view, both the direct fit and the Bayesian approach seem to provide reliable estimate of the SVH parameters. However, the scatter in Table 1 is almost two times larger than the one estimated by the direct fit method. This is an expected result. The two fitting procedures actually minimizes a similar merit function and indeed, in Sect. 5, we have looked for the minimum of Eq.(57) forcing $\sigma_{int} = 0$ and setting to 1 the denominator in the second term. As discussed in D'Agostini (2005), this is likely to bias low the estimate of σ_{int} which is just what we find. Note that the scatter of the data around the best fit line is essentially the same as the intrinsic scatter so that it is fully explained by the sources generating σ_{int} , namely the variation in the halo parameters.

Looking at the Table 1, it is not possible to definitively infer whether the SVH coefficients are filter dependent. On


Figure 4. Best fit curve (according to the Bayesian method) superimposed on the i' filter data for the fit in Eq.(59).

the one hand, the estimates for the different wavelengths are formally not consistent within each other. Nevertheless, the differences are so small that it is hard to say whether they are significant or due to selection effects or some other uncontrolled systematics.

Being an immediate consequence of the virial theorem and our assumptions (37) and (38), we have up to now written the SVH as a relation giving the velocity dispersion as a function of the photometric parameters. However, we can solve Eq.(39) with respect to R_e as:

$$\log R_e = a_e \log \sigma_0 + b_e \log \langle I_e \rangle + c_e \log (n/4) + d \quad (59)$$

with:

$$\begin{cases} a_e = 1/b \\ b_e = -a/b \\ c_e = -c/b \\ d_e = -d/b \end{cases} \quad (60)$$

which can be directly estimated for the different filters from the values in Table 1. A most reliable estimate is, however, obtained by fitting Eq.(59) to the data using the same procedure as above thus obtaining also a value for the intrinsic scatter. The results are reported in Table 2, while Fig. 4 shows the best fit line superimposed to the data in the fiducial i' filter. It is immediate to see that the values in Table 2 are in strong disagreement with the theoretical expecta-

tions based on Eq.(60) and the values in Table 1. This is however by no means a shortcoming of the model, but only an expected consequence of problems with fitting an inverse relation so that we do not discuss anymore this issue.

It is more interesting to note that the scatter in $\log R_e$ is the same as the intrinsic one. Although this could also be somewhat a consequence of neglecting uncertainties on $\log R_e$, it is an intriguing result. Indeed, while in the FP the scatter must be accounted for by both observational errors and intrinsic terms, here the intrinsic scatter is the only source of scatter. Moreover, such an intrinsic scatter is fully related to the variations in the dark matter parameters so that its origin is fully known and (to some extent) predictable provided a reliable $c - M_{vir}$ relation is given.

It is worth wondering how the inverse SVH (59) works as distance indicator. To this aim, we note that the scatter in $\log R_e$ translates into a $\ln 10 \times \sigma_{int,e} \simeq 23\%$ scatter in the distance estimates. Table 4 in Bernardi et al. (2003) reports a collection from literature of various FP determinations with the corresponding scatter on the distance ranging from 13% to 22% so that, taken at face values, increasing the number of parameters with respect to the FP (4 instead of 3 for the SVH vs the FP) does not ameliorate the performances as distance indicator. Some remarks are however in order. First, different determinations rely on different fitting methods. Should we have used the direct fit approach, the scatter in the distance should be reduced to $\sigma \simeq 16\%$ which is smaller than the 20% value obtained by Bernardi et al. (2003) for a SDSS sample comprising 9000 ETGs with $0.01 \leq z \leq 0.3$. A meaningful comparison should therefore rely on the same fitting method and we advocate the use of our Bayesian approach in order to not underestimate the intrinsic scatter. As a second issue, one has also to consider that our sample is made out of all ETGs in the lowZ catalog without any separation in field or clusters objects. It is therefore worth reconsidering the fit and hence the scatter by performing the fit on smaller subsamples separated according to their environment. This is outside the aims of this introductory investigation and will be presented elsewhere.

7 DISCUSSION AND CONCLUSIONS

Early type galaxies may be considered as a homogenous class of objects from many point of views. A further support to this idea is represented by the existence of several interesting scaling relations among their photometric and/or kinematic parameters, the most famous ones being the FP (between $\log \sigma_0$, $\log \langle I_e \rangle$ and $\log R_e$) and the PhP (where $\log \sigma_0$ is replaced by the Sersic index n). In an attempt to look for a unified description of both these relations, we have presented here the *Sersic Virial Hyperplane* (SVH) expressing a kinematical quantity, namely the velocity dispersion σ_0 as a function of the Sersic photometric parameters ($n, R_e, \langle I_e \rangle$). In the usual logarithmic units, such a relation reduces to a hyperplane (i.e., a plane in four dimensions) where all ETG lay with a small thickness as inferred from the low intrinsic scatter σ_{int} . Just as the FJ relation is a projection of the FP and the KR a projection of the PhP, thus we find that both the FP and the PhP are projections of the SVH so that the scatter in these well known relations can be ascribed to neglect one of the SVH variables.

Our derivation of the SVH relies on very few assumptions. First, ETGs are postulated to be in dynamical equilibrium so that the virial theorem applies. Given that ETGs are old systems likely to have formed most of their stellar content and settled their main structural properties at $z \sim 2$ (Merlin & Chiosi 2006), this hypothesis seems to be well founded, at least as a first well motivated approximation. Starting from this premise, the SVH comes out as a consequence of the virial theorem and of Eqs.(37) and (38). The first one relies on an approximated log-linear relation between the model dependent quantity $w(\mathbf{p})/k(\mathbf{p})$ and the Sersic photometric parameters, while the second one assumes the existence of a power-law relation between the stellar M/L ratio Υ_* and the total luminosity L_T . Given mass models for the luminous and dark components of a typical ETG, Eq.(37) has been verified by realistic simulations reproducing the distribution in the photometric parameters of a large ETG sample selected from the low redshift version of the VAGC catalog based on SDSS DR2. On the other hand, the relation $\Upsilon_* \propto L_T^\beta$ is expected on the basis of stellar populations synthesis models and is also invoked to explain the FP tilt. It is worth stressing, however, that here the tilt of the SVH is due to the dependence of the stellar M/L on L_T , while, in the case of the FP, such a relation involve the global (stellar plus dark) M/L ratio. As a consequence, one has to resort to a mechanism coupling the dark and luminous mass density profiles in order to have $M_{dyn}/L_T \propto L_T^\beta$, while here we only rely on what is predicted by stellar population synthesis models. From this point of view, therefore, the SVH relies only on known physics without the need of any unexplained interaction between baryons and CDM particles.

The discussion in Sect. 5 have confidently demonstrated that the observed SVH is consistent with our theoretical predictions so that it is worth wondering how the present introductory work can be ameliorated. To this aim, it is worth reconsidering the derivation of the observed SVH in Sect. 6. Here we have used the Bayesian approach to infer the estimate of the SVH coefficients and its intrinsic scatter from a dataset based on the lowZ catalog. Such a sample is however affected by known problems. First, the automated code used by Blanton et al. (2005) to estimate the Sersic parameters does not work very well. The recovered values of (n, R_e, A) and hence of $\log \langle I_e \rangle$ are biased in a complicated way depending on the values of the parameters themselves. Modeling this bias and taking care of it in the fitting procedure is quite difficult, but the problem should be coped with by checking how it affects the estimate of the SVH coefficients. It is worth stressing, however, that this problem does not impact anyway our testing of the SVH. However, to test the SVH, one has to verify that, for a given distribution of photometric parameters based on a whichever real sample, the simulated sample and the observed one predict the same SVH coefficients which is indeed what we find. Note also that this method allows to automatically include the selection effects in the simulation without the need for accurately modelling them. The data we have used present, however, a second shortcoming, i.e. there is no estimate of the uncertainties on the Sersic photometric parameters. As shown in Eq.(57), these quantities enter the definition of the merit function to be minimized in the Bayesian determination of the SVH coefficients. Although one can estimate what the effect is by artificially attaching measurement errors to

the input quantities, it is more convenient to solve the problem by resorting to a different sample in order to address the problem hinted above. The recently released Millennium Galaxy Catalog (Liske et al. 2003; Driver et al. 2006) contains a detailed bulge/disc decomposition of ~ 10000 nearby galaxies with detailed fitting of the Sersic law to the surface brightness profile (Allen et al. 2006). The code is tested and shown not to be biased and the errors on the photometric parameters are available. Cross-matching with the SDSS and selecting only the ETGs should provide an ideal sample to test the SVH retrieving a more reliable estimate of its coefficients and scatter thus allowing to reconsider it as a distance indicator.

From a theoretical point of view, it is worth reconsidering our basic assumptions. As discussed above, the tilt of the SVH with respect to the virial theorem predictions may be fully ascribed to a power-law relation between the stellar M/L ratio Υ_* and the total luminosity L_T . Although estimating the slope β from the tilt is, in principle, possible, confronting with an expected value is welcome. To this aim, one can resort to stellar population synthesis models (Fioc & Rocca-Volmerange 1996; Bruzual & Charlot 2003; Le Borgne et al. 2005; Maraston 2005) by varying the different ingredients entering the codes and looking (by trial and error) for the combination giving the slope β needed to reproduce the correct SVH tilt. Should these stellar models be able to reproduce the observed colors of ETG, our derivation of the SVH could be further strengthened.

A fundamental role in the ETG modeling has been played by the choice of the dark halo model. Although the NFW mass density profile is the standard one, it is nevertheless well known that it encounters serious difficulties in explaining the inner rotation curves of low surface brightness galaxies (see, e.g., de Blok 2005 and refs. therein). Moreover, some recent evidences from the planetary nebulae dynamics have put into question the need for a significative amount of dark matter in the inner regions of elliptical galaxies (Romanowski et al. 2003; Napolitano et al. 2005). Estimating the dark matter content for the real galaxies is difficult, but we can rely on what we know from the modeling of the simulated galaxies since they reproduce the same SVH as the observed ones. Defining the dynamical mass^{***} M_{dyn} as the total mass within R , i.e. $M_{dyn}(R) = \Upsilon_* L(R) + M_{DM}(R)$, we find a median value $M_{DM}(R_e)/M_{dyn}(R_e) \simeq 14\%$ (with a rms value of 20%) so that inner regions turn out to be baryon dominated as expected. This also makes us confident that changing the halo model does not affect significantly the theoretical values of the SVH coefficients. A subtle effect, worth to be investigated, is the relation between the concentration c and the virial mass M_{vir} of the halo. Actually, the scatter of this relation concurs in determining the scatter in the SVH. Said in another way, for given M_{vir} and stellar mass parameters, the scatter in the $c - M_{vir}$ relation introduces a scatter on $M_{DM}(R_e)/M_{dyn}(R_e)$ thus contributing to the total SVH scatter. Numerical N-body simulations and

semi-analytical galaxy formation models predict different halo models with its own $c - M_{vir}$ relation and scatter. It should be tempting to investigate whether a large ETG sample (free of the problems described above) could be used to discriminate among these different possibilities on the basis of the scatter they predict for the SVH.

The aim of the present paper was mainly to introduce the SVH as a unifying scenario for the ETG scaling relations. If the encouraging results presented here will be further confirmed, both observationally and theoretically, we are confident that the SVH could represent a valid tool to investigate the ETG properties under a single picture.

Acknowledgements. Funding for the Sloan Digital Sky Survey (SDSS) has been provided by the Alfred P. Sloan Foundation, the Participating Institutions, the National Aeronautics and Space Administration, the National Science Foundation, the U.S. Department of Energy, the Japanese Monbukagakusho, and the Max Planck Society. The SDSS Web site is <http://www.sdss.org/>.

The SDSS is managed by the Astrophysical Research Consortium (ARC) for the Participating Institutions. The Participating Institutions are The University of Chicago, Fermilab, the Institute for Advanced Study, the Japan Participation Group, The Johns Hopkins University, Los Alamos National Laboratory, the Max-Planck-Institute for Astronomy (MPIA), the Max-Planck-Institute for Astrophysics (MPA), New Mexico State University, University of Pittsburgh, Princeton University, the United States Naval Observatory, and the University of Washington.

REFERENCES

- Abazajian, K., Adelman-McCarthy, J.K., Agüeros, M.A., Allam, S.S., Anderson, K.S.J., Anderson, S.F. et al. 2004, *AJ*, 128, 502
- Adelman-McCarthy, J.K., Agüeros, M.A., Allam, S.S., Anderson, K.S.J., Anderson, S.F. et al. 2006, *ApJS*, 162, 38
- Akritas, M.G., Bershad, M.A. 1996, *ApJ*, 470, 706
- Allen, P.D., Driver, S.P., Graham, A.W., Cameron, E., Liske, J., de Propris, R. 2006, *MNRAS*, 371, 2
- Bender, R., Burstein, D., Faber, S.M. 1992, *ApJ*, 399, 462
- Bernardi, M., Sheth, R.K., Annis, J., Burles, S., Eisenstein, D.J. et al. 2003, *AJ*, 125, 1866
- Bernardi, M., Sheth, R.K., Nichol, R.C., Schneider, D.P., Brinkmann, J. 2005, *AJ*, 129, 61
- Binney, J., Tremaine, S. 1987, *Galactic Dynamics*, Princeton University Press, Princeton
- Blanton, M.R., Schlegel, D.J., Strauss, M.A., Brinkmann, J., Finkbeiner, D. et al. 2005, *AJ*, 129, 2562
- Bruzual, G., Charlot, S. 2003, *MNRAS*, 344, 1000
- Bullock, J.S., Kolatt, T.S., Sigad, Y., Somerville, R.S., Kravtsov, A.V., Klypin, A., Primack, J.P., Dekel, A. 2001, *MNRAS*, 321, 559
- Busarello, G., Capaccioli, M., Capozziello, S., Longo, G., Puddu, E. 1997, *A&A*, 320, 415
- Caon, N., Capaccioli, M., D'Onofrio, M. 1993, *MNRAS*, 265, 1013
- Cardone, V.F., Piedipalumbo, E., Tortora, C. 2005, *MNRAS*, 358, 1325
- Ciotti, L. 1991, *A&A*, 249, 99
- D'Agostini, G. 2004, *physics/0412148*
- D'Agostini, G. 2005, *physics/0511182*
- Dalal, N., Keeton, C.R. 2003, *astro-ph/0312072*

^{***} Note that here we compute the dynamical mass from the known values of the model parameters rather than estimating it from the velocity dispersion. For this reason, although the definition is the same, our values for M_{dyn} differ from those one would obtain using the formula in Padmanabhan et al. (2005).

- de Blok, W.J.G. 2005, *ApJ*, 634, 227
- de Vaucouleurs, G. 1948, *Ann. d' Astroph.*, 11, 247
- Djorgovski, S., Davis, M. 1987, *ApJ*, 313, 59
- Dressler, A., Lynden - Bell, D., Burstein, D., Davies, R.L., Faber, S.M., Terlevich, R.J., Wegner, G. 1987, *ApJ*, 313, 42
- Driver, S.P., Allen, P.D., Graham, A.W., Cameron, E., Liske, J. 2006, *MNRAS*, 368, 414
- Faber, S., Jackson, R. 1976, *ApJ*, 317, 1
- Feigelson, E.D., Babu, G.J. 1992, *ApJ*, 397, 55
- Fioc, M., Rocca - Volmerange, B. 1997, *A&A*, 326, 950
- Fukugita, M., Shimasaku, K., Ichikawa, T. 1995, *PASP*, 107, 945
- Fukugita, M., Hogan, C.J., Peebles, P.J.E. 1998, *ApJ*, 503, 518
- Ghigna, S., Moore, B., Governato, F., Lake, G., Quinn, T., Stadel, J. 2000, *ApJ*, 544, 616
- Graham, A.W., Colless, M. 1997, *MNRAS*, 287, 221
- Graham, A.W. 2002, *MNRAS*, 334, 859
- Graham, A.W., Driver, S.P. 2005, *PASA*, 22, 118
- Graham, A.W., Merritt, D., Moore, B., Diemand, J., Terzic, B. 2006a, *AJ*, 132, 2701
- Graham, A.W., Merritt, D., Moore, B., Diemand, J., Terzic, B. 2006b, *AJ*, 132, 2711
- Jørgensen, I., Franx, M., Kjaergaard, P. 1995, *MNRAS*, 273, 1097
- Jørgensen, I., Franx, M., Kjaergaard, P. 1996, *MNRAS*, 280, 167
- Kauffman, G., Heckman, T.M., White, S.D.M., Charlot, S., Tremonti, C. et al. 2003, *MNRAS*, 341, 33
- Khosroshahi, H.G., Wadadekar, Y., Kembhavi, A., Mobasher, B. 2000, *ApJ*, 531, L103
- Kormendy, J. 1977, *ApJ*, 218, 333
- La Barbera, F., Busarello, G., Capaccioli, M. 2000, *A&A*, 362, 851
- La Barbera, F., Merluzzi, P., Busarello, G., Massarotti, M., Mercurio, A. 2004, *A&A*, 425, 797
- La Barbera, F., Covone, G., Busarello, G., Capaccioli, M., Haines, C.P., Mercurio, A., Merluzzi, P. 2005, *MNRAS*, 358, 1116
- Le Borgne, D., Rocca - Volmerange, B., Prugniel, P., Lancon, A., Fioc, M., Soubiran, C. 2005, *A&A*, 425, 881
- Lima Neto, G.B., Gerbal, D., Márquez, I. 1999, *MNRAS*, 309, 481
- Liske, J., Lemon, D.J., Driver, S.P., Cross, N.J.G., Couch, W.J. 2003, *MNRAS*, 344, 307
- Maraston, C. 2005, *MNRAS*, 362, 799
- Márquez, I., Lima Neto, G.B., Capelato, H., Durret, F., Lanzoni, B., Gerbal, D. 2001, *A&A*, 379, 767
- Mazure, A., Capelato, H.V. 2002, *A&A*, 383, 384
- Merlin, E., Chiosi, C. 2006, *A&A*, 457, 437
- Merritt, D., Graham, A.W., Moore, B., Diemand, J., Terzic, B. 2005, *astro-ph/0509417* (*AJ* in press)
- Moore, B., Governato, F., Quinn, T., Stadel, J. 1998, *ApJ*, 499, L5
- Moore, B., Ghigna, S., Governato, F., Lake, G., Quinn, T., Stadel, J., Tozzi, P., 1999, *ApJ*, 524, L19
- Napolitano, N.R., Capaccioli, M., Romanowsky, A.J., Douglas, N.G., Merrifield, M.R., Kuijken, K., Arnaboldi, M., Gerhard, O., Freeman, K.C. 2005, *MNRAS*, 357, 691
- Navarro, J.F., Frenk, C.S., White, S.D.M. 1997, *ApJ*, 490, 493
- Navarro, J.F., Hayashi, E., Power, C., Jenkins, A.R., Frenk, C.S. et al. 2004, *MNRAS*, 349, 1039
- Noordermeer, E., van der Hulst, J.M., Sancisi, R., Swaters, R.S., van Albada, T.S. 2007, *astro-ph/0701731*
- Padmanabhan, N., Seljak, U., Strauss, M.A., Blanton, M.R., Kauffman, G. et al. 2004, *New Astron.*, 9, 329
- Prugniel, Ph., Simien, F. 1997, *A&A*, 321, 111
- Roscoe, D.F. 1999, *A&A*, 343, 788
- Romanowsky, A.J., Douglas, N.G., Arnaboldi, M., Kuijken, K., Merrifield, M.R., Napolitano, N.R., Capaccioli, M., Freeman, K.C. 2003, *Science*, 301, 1696
- Sersic, J.L. 1968, *Atlas de Galaxies Australes*, Observatorio Astronómico de Córdoba
- Shimasaku, K., Fukugita, M., Doi, M., Hamabe, M., Ichikawa, T. et al., 2001, *AJ* 122, 1238
- Trujillo, I., Bukert, A., Bell, E.F. 2004, *ApJ*, 600, L39
- van der Marel, R. 1991, *MNRAS*, 253, 710
- Young, C.K., Currie, M.J. 1994, *MNRAS*, 268, L11